Spectroscopic investigation of oxidation in GaSe 2D layered materials

Badreddine Smiri, Rémy Bernardin, Mickael Martin, Hervé Roussel, Jean Luc Deschanvres, Emmanuel Nolot, Névine Rochat, Franck Bassani, Thierry Baron, Bernard Pelissier

Spectroscopic Investigation of Oxidation in GaSe 2D Layered Materials: Understanding the Evolution and Mechanisms"

Badreddine Smiri[1,2,3], Rémy Bernardin[1], Mickael Martin[1], Hervé Roussel[3], Jean Luc Deschanvres[3], Emmanuel Nolot[2], Névine Rochat[2], Franck Bassani[1], Thierry Baron[1], Bernard Pelissier[1*]*

[1]Univ. Grenoble Alpes, CNRS, CEA/LETI Minatec, Grenoble INP, LTM, 38000 Grenoble, France
[2]Univ. Grenoble Alpes, CEA, LETI, 38000 Grenoble, France
[3]Univ. Grenoble Alpes, CNRS, Grenoble INP, LMGP, F-38000 Grenoble, France

a) Authors to whom correspondence should be addressed:
badreddine.smiri@cea.fr & bernard.pelissier@cea.fr

Abstract:

GaSe, a two-dimensional layered metal monochalcogenide, has recently attracted growing interest due to its unique electronic properties and potential technological applications. In this study, we investigate the oxidation mechanisms and properties of GaSe exposed to air for different durations, using a combination of Raman spectroscopy, atomic force microscopy (AFM), photoluminescence (PL), and X-ray photoelectron spectroscopy (XPS). The Raman analysis reveals the oxidation of GaSe, resulting in the formation of a thin layer comprising Ga_2Se_3, Ga_2O_3, and amorphous selenium. Utilizing these signatures, oxidation is then tracked. Through a comprehensive study involving diverse laser excitations, polarization configurations, and resonant Raman techniques, we emphasize the crucial utility of Raman methods as rapid, non-destructive characterization tools—ideal for continuous monitoring of oxidation processes. This exploration indicates an immediate oxidation response in GaSe layers upon exposure to air. Following oxidation, the ultrathin GaSe photoluminescence (PL) and Raman intensity undergo a rapid decline, linked to reduction in GaSe thickness. By investigating penetration depths using various Raman excitation wavelengths, we achieve a layer-specific characterization of our sample. This finding is important for the understanding and application of GaSe 2D materials.

KEYWORDS: Raman spectroscopy, GaSe, 2D materials, oxidation, aging.

Introduction

The exploration of two-dimensional van der Waals (2D-vdW) materials, with a focus on diatomic-layered GaSe, has sparked profound interest within the scientific community, opening avenues for innovations in electronic and optical technologies.[1–3] The quality and performance of 2D materials are significantly influenced by the presence of disorder, stemming from both intrinsic factors like

crystalline defects and extrinsic factors such as environmental contaminants. The principal sources of intrinsic and extrinsic disorder in 2D materials encompass strain, adsorbates, surface roughness, charged impurities within the substrate, and defects induced oxidation. This influence is particularly pronounced in 2D systems, given their inherent surface nature, making them highly susceptible to external sources of disorder.

These materials have a wide-band gap variation, and great light absorption. The photoelectric characteristics of GaSe are notably influenced by its layer thickness. GaSe exhibits a direct band gap of 2.1 eV in bulk, while its monolayer form has an indirect band gap of 4 eV.[4,5] GaSe thickness of each atomic monolayer is 0.93 nm and a lattice constant of 0.374 nm, composed of a repeating sequence of four atoms arranged as Se-Ga-Ga-Se.[6] Within the interlayer planes, GaSe displays strong ionic bonding, while vdW forces govern the bonding between interlayer planes. The difference in stacking sequences among the interlayers in the out-of-plane direction contributes to its phase diversity, including β-GaSe: 4 D6h, γ-GaSe: C3v, δ-GaSe: C6v, and ε-GaSe: D3h phases .[6,7] Some crystalline polytypes of GaSe are known to show strong nonlinear optical behaviour attributed to the absence of inversion symmetry.[7–9] The surge of interest in layered materials has propelled remarkable progress in the fields of photonics, electronics, and spintronics.[5,8,10–12] However, the inherent susceptibility of 2D GaSe materials to oxidation poses a formidable challenge.

Exposure to air triggers chemical reactions between these materials and oxygen, leading to the formation of undesirable oxide coatings on their surfaces. This oxidation process can lead to deterioration in electrical, structural, and optical properties, significantly hindering their practical applications.[10,13] This challenge necessitates the implementation of stringent material quality control measures throughout the integration process to ensure the optimal performance of 2D GaSe materials.

Raman spectroscopy is a powerful tool to investigate oxidation process and to determine the number of layers of 2D Materials (GaSe, WS_2, MoS_2, Graphene…).[13–17] By analyzing the vibrational modes of the material, Raman spectroscopy can provide valuable insights into the structural changes induced by oxidation. This technique allows for non-destructive and rapid characterization, making it ideal for monitoring the oxidation process in real-time. Raman spectroscopy has been playing an important role to investigate the GaSe properties in terms of thickness in the last half decade.[6,7,18] Hence, Raman spectroscopy under resonance conditions

enables a deeper understanding of 2D materials physical properties. By selecting an excitation laser that matches the electronic transitions in materials, resonance Raman spectroscopy enhances the Raman signal and provides more detailed information about the material's vibrational modes. This technique allows for the investigation of specific electronic states and their coupling with lattice vibrations, revealing valuable insights into the material's electronic structure, structural and optical properties. Previous studies investigating GaSe oxidation have produced much controversial results. Some researchers,[13,19,20] through the use of Raman and XPS, have exclusively identified gallium oxides as the primary products of GaSe oxidation. More detailed experimental work is required to propose an in-depth mechanism of oxidation.

In this study, we examine the oxidation dynamics of ultrathin GaSe when exposed to ambient conditions for varying durations. Using Raman scattering, AFM, XPS and PL spectroscopies, we investigate the vibrational, structural and optical properties of GaSe crystal during oxidation. These discoveries will contribute to the study of oxidation mechanisms and the development of 2D GaSe materials for practical applications.

1. EXPERIMENTAL SECTION

GaSe layers were grown on standard Crystalwise 2in C-plane sapphire wafer. Growth were made by a process adapted from[21] and was done in a 300mm MOCVD reactor from Applied Material. The substrate where hold on a SiC coated graphite 2inches to 300mm holder. Substrate preparation is limited to an annealing step (20torr – 600s – 885°C – H2 atmosphere). This annealing step was shown to have a negligible influence on the surface structure as no terrace/step formation was observed in previous experiments. The precursors are TMGa and DiPSe with an H2 laminar flux as carrier gaz. The growth recipe was composed of two main steps. (1) A nucleation step, (2) A 500s lateral growth step of the step (1) nuclei. Step (2) condition should inhibit nucleation on the sapphire substrate. Hence allowing to have a pure lateral growth of GaSe from the step (1) nuclei. However, further analysis show that it might not be the case and that some amount of nucleation would appear at this step. It should be noted that significant vertical growth is observed during this step - due to the screw-dislocation driven growth mode. The GaSe layer is fully coalesced (fig 1.a) and a preferential orientation of the GaSe domain can be seen easily in the upper GaSe layers of our sample (fig 1.b). Orientation of the subsequent layers are not as easily seen because of the AFM image quality but are assumed to be the same.

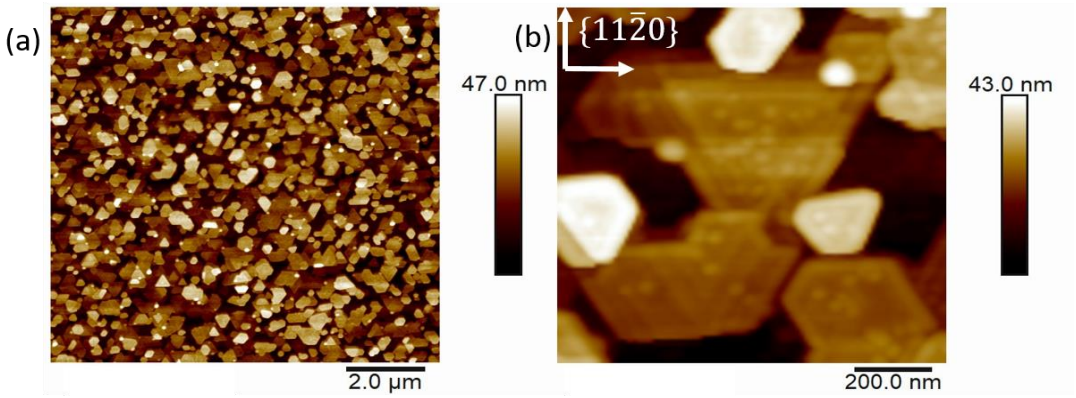

Figure 1: a) AFM image of a GaSe layers grown on C-sapphire (Al_2O_3) substrate; b) Detailed views of the GaSe flake – sapphire orientation is given and show the general preferred orientation.

Various characterization techniques were used to analyze the oxidation dynamics of GaSe exposed in ambient atmosphere. Surface morphology has been studied with an AFM (Bruker Dimension Icon; OTESPA-R3 silicon tips) in tapping mode. Multiple measurements were made at different time of the oxidation process.

Raman measurements were performed on several confocal Raman systems (LabAM Soleil, customized LabRAM HR from Horiba Jobin Yvon, and in Via from Renishaw) in backscattering configuration using a 355 nm UV laser and three visible lasers at 473, 532 and 633 nm. In UV experiments, the laser light was focused on the sample using an objective lens (0.5 N.A., 60×). In the visible light experiments, the laser light was focused on the sample surface through a 100× objective lens (0.95 N.A.). The scattered light was collected and dispersed using a spectrometer equipped with a CCD camera. To avoid heating effects, the power of all laser lines used was below 1 mW. The laser spot size was set at 1 µm. Polarized Raman experiments include different configurations, namely $z(yx)\bar{z}$ and $z(yy)\bar{z}$ c, where the first symbol represents the input polarization and the second represents the output polarization. In the $z(yx)\bar{z}$ configuration, the incident light passes through the half-wave plate and the returning light is collected by the polarizer. Similarly, in the $z(yy)\bar{z}$ configuration, the incident light passes through the half-wave plate, and the return light is collected after passing through the polarizer and half-wave plate. PL spectra were obtained on a LabRAM soleil Raman system with 150 lines/mm grating and a 532 nm excitation laser.

XPS (X-ray Photoelectron Spectroscopy) measurements have been carried out on a customized parallel angle resolved (pARXPS) Theta 300 from Thermo Fisher Scientific operating under ultrahigh vacuum conditions (10^{-9} mbar), alongside a monochromized Al Kα1,2 x-ray source

emitting at 1486.6 eV. Parallel angle resolved spectra were simultaneously collected without any sample tilt and with an incident angle ranging from 23.75 to 76.25° with respect to the sample's surface normal.

The Fitspy 2023.5 program, developed by Quéméré et al[22] at CEA Grenoble, is a versatile Python tool designed for spectrum fitting. It features a user-friendly GUI to ensure ease of use. This program is primarily utilized for handling spectral data and conducting curve fitting. The spectral bands are fitted using a pseudo-Voigt line shape, which combines Gaussian and Lorentzian functions, along with a polynomial baseline correction.

2. RESULTS AND DISCUSSION

Figure 2 shows the Raman spectra for a GaSe crystal surface exposed in ambient atmosphere for various time periods for the same sample. Raman spectroscopy was used to measure the fingerprints of GaSe. The Raman spectra of GaSe exhibit four prominent peaks at 213, 248, 135 and 307 cm^{-1}, which primarily correspond to the in-plane modes E''(2) and E'(2), as well as the out-of-plane modes A'1(1) and A'1(2).[19,23,24] In addition to the Raman modes associated with GaSe, additional peaks were detected at 159, 166, 262 and 294 cm^{-1}, resulting from the oxidation mechanisms. The oxidation process of GaSe can be explained by two primary reactions[20], $12GaSe+3O_2 \rightarrow 4.Ga_2Se_3+2.Ga_2O_3$ and $4.GaSe+3.O_2 \rightarrow 2.Ga_2O_3+4.Se$ During these reactions, selenium atoms are replaced by oxygen atoms resulting in the formation of amorphous selenium in conjunction with the oxide.

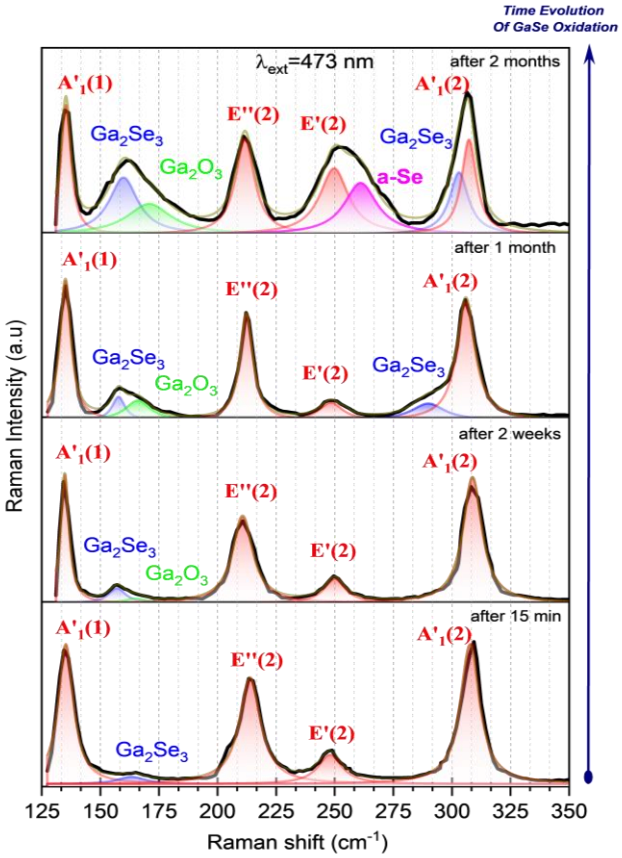

Figure 2: Raman spectra of the GaSe crystal surface exposed in an ambient atmosphere for various time periods indicated in the graph.

After peak fitting using Fitspy, the compounds, Ga_2Se_3, Ga_2O_3, and Amorphous selenium (a-Se), are identified. a-Se exhibits a wide Raman peak at approximately 262 cm^{-1},[13] while Ga_2Se_3 is

clearly identified by broad peaks at 159 and 294 cm^{-1}.[13,25,26] Yet, the broad peak at 159 cm^{-1} corresponds to the A1 mode of ordered Ga_2Se_3.[25] Furthermore, it could be speculated from the calculation made by Finkman et al,[27] that the broad peak at 294 cm^{-1} originates from the TO branches of Ga_2Se_3. There is also a peak at around 167 cm^{-1} in the spectra of the oxidized samples, which corresponds to the most powerful phonon mode of Ga_2O_3.[28]

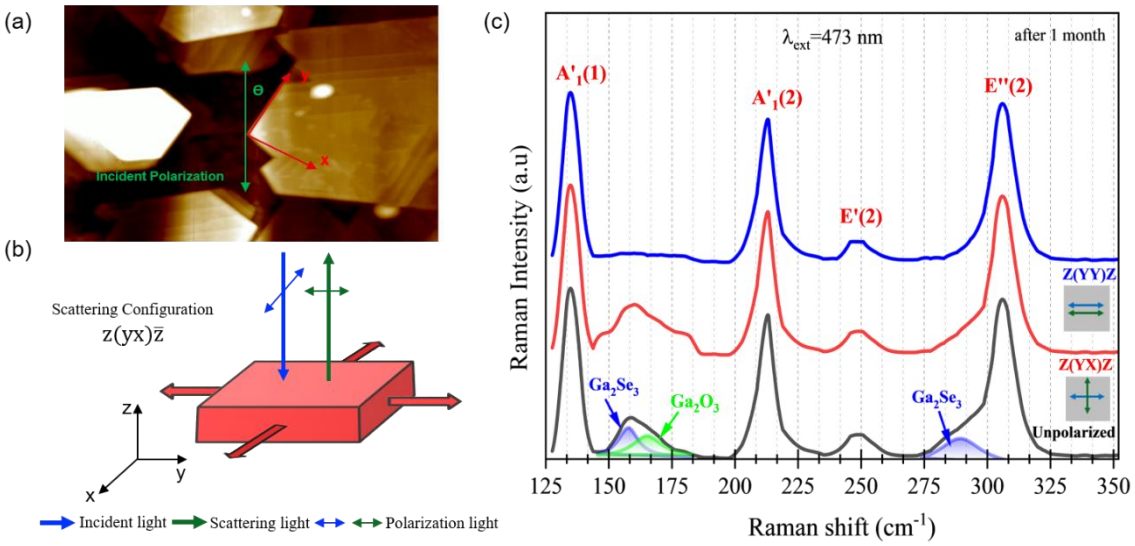

Figure 3: a) AFM image of the GaSe sample. θ is defined as the angle between the y-axis of GaSe and the incident polarization. b) Schematic of the polarized Raman configuration. The incident and scattered light propagates along the crystalline z-axis, and their polarizations are varied within the xy plane c) Raman spectra of GaSe crystal surface exposed in an ambient atmosphere after 1 month measured in different polarization configurations measured with 473 nm excitation wavelength.

To gather more information about the oxidation product peaks, we conducted a somewhat complex study using polarized Raman spectroscopy. Raman spectroscopy measurements were performed using two polarization configurations (parallel, ⇳→⇳, versus crossed, ⇳→ ⇔), as shown in figure 3b. All spectra discussed later will be described by notations of the type $z(yx)\bar{z}$, according to Porto's notation.[29] The Raman spectra taken in backscattering geometry are shown in figure 3c. The results revealed a significant difference in the obtained spectra, particularly regarding the presence of peaks corresponding to oxidation products. In the $z(yy)\bar{z}$ configuration (parallel, ⇳→⇳), where the laser and detector were aligned perpendicularly, peaks of the oxidation products Ga_2Se_3 and Ga_2O_3 were clearly observed in the Raman spectrum. Conversely, these peaks were absent in the $z(yx)\bar{z}$ configuration (crossed, ⇳→ ⇔). This observation suggests a dependence of the oxidation product detection on the polarization configuration used. In the cross-polarized

configuration shown in figure 3b, only the Ga_2O_3 and Ga_2Se_3 modes are allowed. This is because the form of the Raman tensors imposes selection rules, which means that Raman modes of specific symmetries can be extinguished for certain polarization configurations.[30]

The explanation for this difference likely lies in the specific interaction between the incident laser and the vibrations of the oxidation products, which can vary depending on the system's polarization. The $z(yy)\bar{z}$ configuration appears to promote a stronger interaction between the laser and the vibrations of the oxidation products, leading to their observation in the Raman spectrum.

This dependency of the oxidation products peaks with the laser polarization suggests that the Ga_2O_3 oxyde layer tends to an oriented structural state with time. It is important to note that these oxidation peaks and behavior under polarization are not seen for GaN layer oxidation,[31–33] leading us to suggest here a mechanism linked with the intrinsic GaSe structure. However, considering the native nature of this oxide growth, this effective result on Raman spectra has to be investigated more deeply. Some GIXRD at very low grazing incidence angle have been performed and the pics identification is on going.

The formation of these oxidation products have been monitored over time by observing the changes in the intensity of their Raman modes. Figure 2 shows that the relative integrated intensity of all GaSe modes decreases with time. After exposure of 2 weeks and more, the Raman signal of GaSe is dominated by two even broader features. After two months of exposure to air, the ratio of Raman intensities between GaSe and Ga_2Se_3 decreased to 55% of its initial value. This significant reduction indicates that the oxidation process has severely compromised the integrity of the GaSe layer. In addition, PL measurements have shown that the luminescence intensity measured at 620 nm also decreases (see figure 7). Our findings suggest that only the uppermost layer of the GaSe material has undergone oxidation, resulting in a layered structure composed of an ultrathin GaSe layer topped by a mix of Ga_2Se_3, a-Se, and Ga_2O_3. These findings demonstrate the value of following the changes in Raman peaks and evaluating the intensity ratio in order to accurately assess the degree of oxidation in GaSe samples, which is much less studied in the literature.[26,30] It is obvious that the ratio of intensity between the GaSe A'1(2) and the Ga_2Se_3 peak decreases over time. Considering that Raman mode intensity is directly related to the probed volume of the material for a given Raman absorption mode, we can deduce that the effective thickness of GaSe gradually decreases due to oxidation. When GaSe is oxidized, layers of Ga_2O_3 are formed on the GaSe surface, this reducing the effective thickness of GaSe. The morphology of the GaSe surfaces

after Raman spectra acquisition at different times (15 min to four months) are presented in figure 4. It has been shown that when GaSe oxidation is important enough, one should be able to see small protrusion at the surface of the GaSe domain.[13] These small protrusions arise around the same time than the prominent 250 cm^{-1} peak from a-Se. The present samples do show the same kind of small protrusions that arise from the GaSe layer dissociation. Raman spectroscopy provides compelling evidence confirming the ongoing oxidative process in GaSe, aligning seamlessly with our observations.

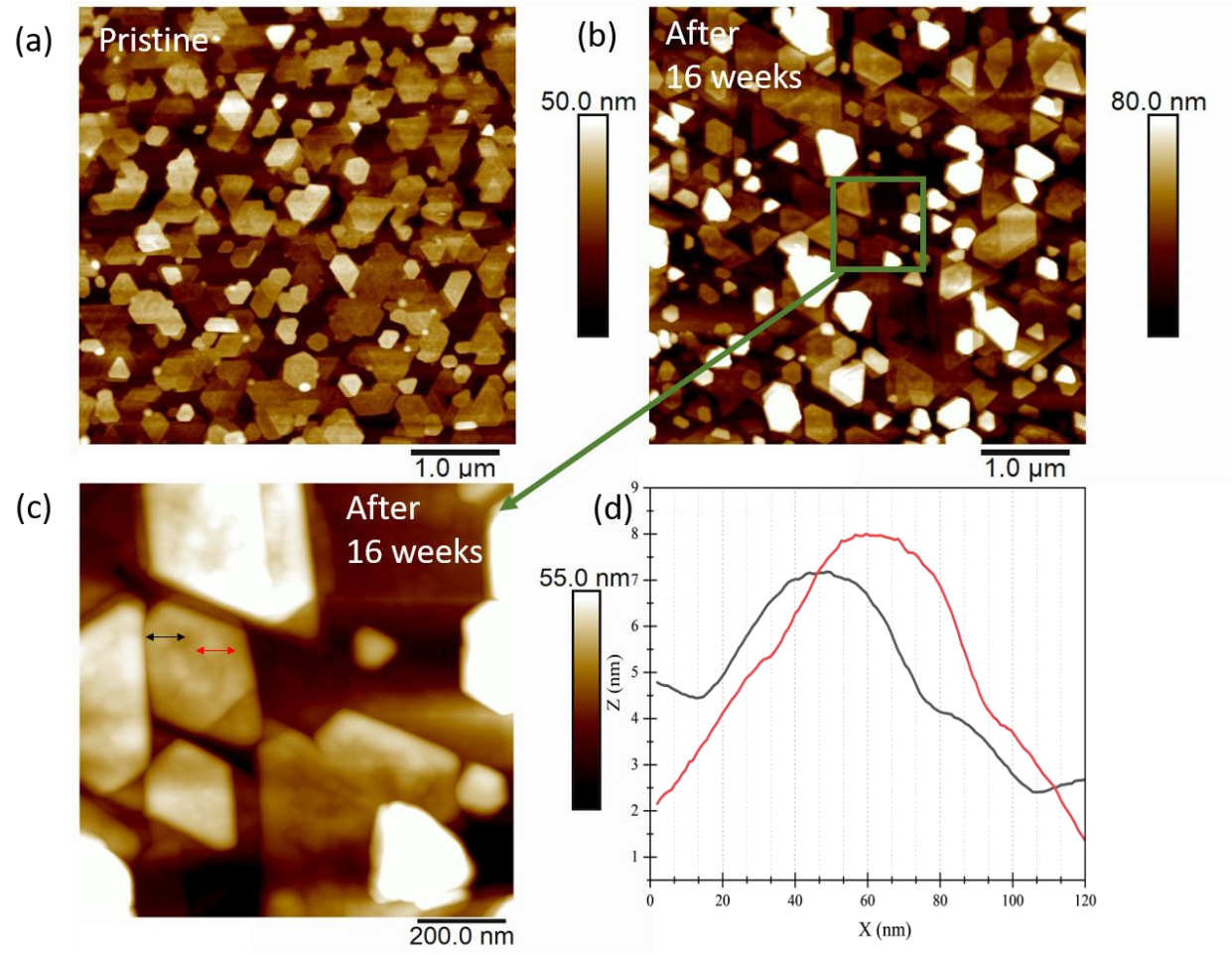

Figure 4: a) AFM surface morphology after epitaxial growth; b) Same sample after 16 weeks at atmosphere; c) Zoom-in of the surface – small protrusions can be easily seen; d) Cross-section profile of two of the small protrusions.

For a more detailed study of the effect of oxidation and the physical properties of GaSe, we used different wavelength for the excitation laser. In this way, we can probe different depths of the GaSe sample, leading to a more comprehensive view of its properties and structure. The variation in excitation wavelengths provides information about the distribution of vibrational modes, chemical composition, and crystal symmetry at different depths.[14,34–36] In fact, when using a 355 nm laser excitation as shown in figure 5, the penetration depth is relatively shallow. This is due to increased light scattering by the surface layers at this wavelength. As a result, the laser beam primarily interacts with the surface layers, allowing clear observation of the Raman peaks corresponding to Ga_2O_3, a-Se, and Ga_2Se_3. This provides specific information about the molecular vibrations and structural characteristics of these materials. On the other hand, using a laser excitation wavelength greater than 514 nm increases the penetration depth of the laser into the sample.[37] The light at this wavelength can reach deeper layers of the sample, reducing the interaction with the surface layers. As a result, the Raman peaks associated with Ga_2O_3, a-Se, and Ga_2Se_3 may be absent or less intense.

Interestingly, its Raman spectrum with 633 nm laser excitation shows an additional strong peak located near 252 cm^{-1}, accompanied by a shoulder at approximately 244.0 cm^{-1}. Notably, this peak was not clearly observed when excited by other laser wavelengths, as shown in figure 5. It is believed that the 252 cm^{-1} peak corresponds to the E'2 mode, which is specific to the D3h-symmetric GaSe structure (ε-phase), and it is in good agreement with previous literature reports.[38,39] On the other hand, the intensity of the common Raman modes (E"(2), A'1(1) and A'1(2)) in all samples was reduced. Previous research has suggested that the appearance of unusual Raman active modes between 244 cm^{-1} and 252 cm^{-1} is attributed to a first-resonant Raman (FRR) scattering process.[40,41] The first-

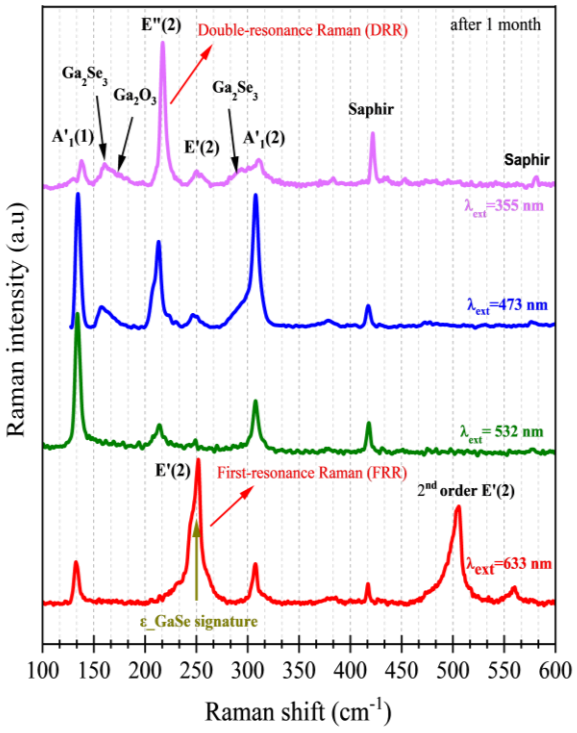

Figure 5: Raman spectra of GaSe taken by various laser excitation wavelengths: (pink) 355 nm, (blue) 473 nm; (green) 532 nm; (red) 633 nm.

order Raman scattering only allows the observation of phonons at the Brillouin zone center (the Γ point). Therefore, the optical transitions can be regarded as strictly vertical. This occurs when the energy of the laser excitation nearly matches the electronic transition energy of the material. In addition, consistent with other publications,[42] the distinguishing feature between the Raman spectra of β-GaSe and ε-GaSe is the presence of an additional mode at about 252 cm^{-1}. The findings provided clearly confirms the ε-phase dominance in our GaSe epitaxial layers. The specific Raman modes observed and their absence under other excitation wavelengths provide substantial evidence for the prevalence of the ε-phase in the studied GaSe samples. Furthermore, we performed X-ray diffraction (XRD) measurements. We observe the superposition of peaks corresponding to β-GaSe and ε-GaSe phases. Therefore, determining the GaSe phase by XRD alone is challenging due to overlapping peaks of different phases. On the other hand, the Raman spectrum obtained with a 355 nm laser excitation reveals the predominance of the E"(2) peak around 216 cm^{-1}. This excitation wavelength corresponds to high optical absorption in GaSe. As a consequence, we see that the double resonance Raman (DRR) scattering mechanism has a considerable influence.[36]

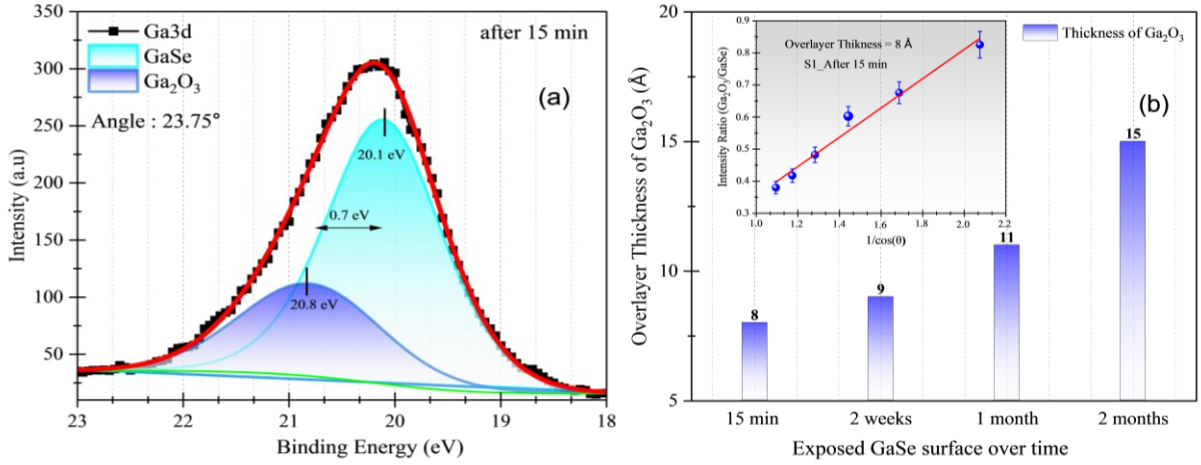

Figure. 6: (a) Typical XPS fit of the Ga3d energy level. The measurement corresponds here to the 15 min air exposure. b) Plot of the measured thicknesses of Ga_2O_3 versus air exposure durations. The insert shows the thickness measurement obtained from the angular response, which allowing more robust and reliable results.

To provide additional confirmation of our conclusions derived from the Raman and AFM experiments, we performed XPS measurements in order to access to the thickness of the Ga_2O_3 oxide layer that forms on the GaSe surface due to air exposure over time. Thus, the Ga3d energy level was considered and fitted carefully using the parameters previously determined in previous

studies.[43,44] Thus a 0.7 eV split was used between the oxide component and the GaSe "Bulk" component and a typical fit example is given figure 6.a. Thanks to the parallel Angle resolved capability, 8 photoemission angles ranging from 23.75 to 76.25° have been acquired at the same time. In order to evaluate the Ga_2O_3 layer thickness, the slope of the angle response has been fitted (cf. figure 6.b). Better than considering only one photoemission angle like for classical XPS measurement, this Angle based measurement leads to a better reliability and robustness of the measured value.[45] Moreover, the very good alignment of the angular response validates the fit model and evidences the low surface roughness of the oxide layer. The Cumpson–Seah[46] method has been used for the electron mean free paths calculation. Thus, it is worth to note that the absolute thickness value resulting from the calculation is questionable, as it is model-based, and maybe not fully accurate considering such new 2D material. Nevertheless, the relative evolution of the measured thicknesses is clearly reliable. The resulting Ga_2O_3 thickness measurements over time are plotted in figure 6b. The global trend of the thickness increase of the Ga_2O_3 layer is fully consistent with Raman observations. But one can note that the 15 min point XPS measurement value suggests a clear presence of Ga_2O_3 layer whereas the GaSe oxidation products are not evidenced on the Raman spectra. This difference can be attributed to the fact that XPS is sensible to all kinds of Ga-O bonds compared to Raman spectroscopy. Figure 6b reveals that the Ga_2O_3 thickness is 0.8 nm after only 15 minutes of air exposure, increasing to 1.6 nm after 2 months. This nearly twofold growth aligns with the Raman intensity analysis, which has decreased to 55% of its initial value after 2 months of exposure.

The remaining GaSe layer thickness after oxidation can be estimated by considering the frequency difference between peaks A'1(1) and A'1(2), as shown in figure 2. Our results indicate that the thickness of the GaSe_ after exposure of 15 minutes is approximately 12 monolayers (ML), whereas the GaSe_ after exposure of 2 weeks is estimated to be about 10ML thick. The GaSe_ after exposure of 1 month measures around 8 ML, while the GaSe_ after exposure of 2 months is approximately 6ML in thickness. It's important to note that the margin of measurement error is approximately ±2 ML. This reduction in the thickness of the GaSe crystal surface and the luminescence over time when exposed to the ambient atmosphere is confirmed and evaluated using PL techniques in the next section.

Figure 7 shows the PL spectra of GaSe crystal surface being exposed in an ambient atmosphere for various time periods at 300 K using a continuous-wave laser with a wavelength of 532 nm and an excitation power density of 0.3W/cm^2. Figure 7 reveals a reduction in luminescence intensity and an increase in FWHM for GaSe after 2 months of exposure, indicating a degradation in both optical and structural quality. The FWHM increases from 11 meV after 15 minutes of exposure to 17 meV after 2 months of exposure. This degradation is further supported by the observed broadening of the luminescence distribution and a loss of crystallinity. These findings highlight the susceptibility of GaSe to photodegradation and its limitations for long-term optoelectronic applications.[42,47] Additionally, an approximate 20 meV blue-shift in the GaSe peak energy indicates a decrease in GaSe thickness due to oxidation.[3,39] This is in a very good agreement with the Raman spectroscopy results, offering a comprehensive characterization of the impact of oxidation on the properties of GaSe material.

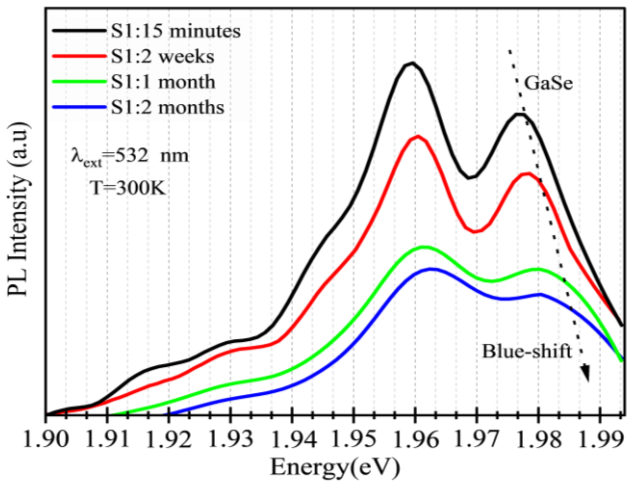

Figure 7: PL spectra of the GaSe crystal surface exposed in an ambient atmosphere for various time periods measured with 532 nm excitation wavelength.

By shedding light on the role of Raman spectroscopy and complementary techniques in monitoring the oxidation of GaSe 2D materials, this study aims to contribute to the development of strategies for enhancing their stability and advancing their applications in various fields.

Conclusion

In summary, a strong dependence of the Raman spectrum and properties of GaSe exposed to air on the oxidation effect is observed and analyzed by a combination of analytical techniques including Raman spectroscopy, AFM, PL, and XPS. Raman spectroscopy emerged as a crucial tool, enabling real-time insights into the structural and optical changes induced by oxidation in 2D GaSe materials. This highlights the non-destructive nature of Raman spectroscopy, making it an invaluable tool for monitoring the stability and integrity of 2D materials in air and during integration processes.

The complexity of GaSe oxidation, driven by factors such as oxygen and humidity results in the formation of a diverse range of oxidation products, including Ga_2Se_3, Ga_2O_3, and a-Se. XPS analysis enabled the estimation of Ga_2O_3 thickness, while PL measurements demonstrated an energy shift correlated with the thickness and degradation in GaSe luminescence under oxidation. AFM imaging revealed the granular morphology of a-Se. The dynamic changes observed in the oxidation products, in conjunction with the reduction of PL and Raman intensity, highlight the interplay between GaSe oxidation and its optical properties. The present results may be also applicable to other 2D semiconducting layered materials.

Conflict of Interest: The authors declare no competing financial interest.

Acknowledgments: This work has been partially supported by the LabEx Minos ANR-10-LABX-55-0 and partially supported by the CNRS RENATECH network.

Reference

1. Li, X. *et al.* Van der Waals Epitaxial Growth of Two-Dimensional Single-Crystalline GaSe Domains on Graphene. *ACS Nano* **9**, 8078–8088 (2015).

2. Mudd, G. W. *et al.* The direct-to-indirect band gap crossover in two-dimensional van der Waals Indium Selenide crystals. *Sci Rep* **6**, 39619 (2016).

3. Terry, D. J. *et al.* Infrared-to-violet tunable optical activity in atomic films of GaSe, InSe, and their heterostructures. *2D Mater.* **5**, 041009 (2018).

4. Feng, Q. *et al.* Strain-tunable band alignment and band gap of GaSe/WTe2 heterojunction for water splitting and light-emitting. *Results in Physics* **28**, 104605 (2021).

5. Rybkovskiy, D. V. *et al.* Size-induced effects in gallium selenide electronic structure: The influence of interlayer interactions. *Phys. Rev. B* **84**, 085314 (2011).

6. Hu, P., Wen, Z., Wang, L., Tan, P. & Xiao, K. Synthesis of Few-Layer GaSe Nanosheets for High Performance Photodetectors. *ACS Nano* **6**, 5988–5994 (2012).

7. Rahaman, M. *et al.* Vibrational properties of GaSe: a layer dependent study from experiments to theory. *Semicond. Sci. Technol.* **33**, 125008 (2018).

8. Karvonen, L. *et al.* Investigation of Second- and Third-Harmonic Generation in Few-Layer Gallium Selenide by Multiphoton Microscopy. *Sci Rep* **5**, 10334 (2015).

9. Allakhverdiev, K. R., Yetis, M. Ö., Özbek, S., Baykara, T. K. & Salaev, E. Yu. Effective nonlinear GaSe crystal. Optical properties and applications. *Laser Phys.* **19**, 1092–1104 (2009).

10. Tonndorf, P. *et al.* Single-photon emitters in GaSe. *2D Mater.* **4**, 021010 (2017).

11. Ke, C. *et al.* Stress engineering on the electronic and spintronic properties for a GaSe/HfSe2 van der Waals heterostructure. *Appl. Phys. Express* **12**, 031002 (2019).

12. Zhou, B. *et al.* A type-II GaSe/GeS heterobilayer with strain enhanced photovoltaic properties and external electric field effects. *Journal of Materials Chemistry C* **8**, 89–97 (2020).

13. Beechem, T. E. *et al.* Oxidation of ultrathin GaSe. *Applied Physics Letters* **107**, 173103 (2015).

14. Lee, C. *et al.* Anomalous Lattice Vibrations of Single- and Few-Layer MoS_2. *ACS Nano* **4**, 2695–2700 (2010).

15. Cadot, S. *et al.* Low-temperature and scalable CVD route to WS2 monolayers on SiO2/Si substrates. *Journal of Vacuum Science & Technology A* **35**, 061502 (2017).

16. Mouloua, D. *et al.* One-step chemically vapor deposited hybrid 1T-MoS2/2H-MoS2 heterostructures towards methylene blue photodegradation. *Ultrasonics Sonochemistry* **95**, 106381 (2023).

17. Mouloua, D. *et al.* Broadband photodetection using one-step CVD-fabricated MoS2/MoO2 microflower/microfiber heterostructures. *Sci Rep* **12**, 22096 (2022).

18. Lei, S. *et al.* Synthesis and Photoresponse of Large GaSe Atomic Layers. *Nano Lett.* **13**, 2777–2781 (2013).

19. Hong, T.-J. *et al.* Snapshots of Ambient Aging in 2D-Layered GaSe. *ACS Appl. Electron. Mater.* **4**, 3049–3055 (2022).

20. Rehman, S. *et al.* Optically Reconfigurable Complementary Logic Gates Enabled by Bipolar Photoresponse in Gallium Selenide Memtransistor. *Advanced Science* **10**, 2205383 (2023).

21. Martin, M. *et al.* 200 mm-scale growth of 2D layered GaSe with preferential orientation. *APL Materials* **10**, 051106 (2022).

22. *Quéméré, P. et al, Fitspy: A Python package for spectral decomposition, Journal of Open Source Software (submitted).*

23. Usman, M. *et al.* Raman Scattering and Exciton Photoluminescence in Few-Layer GaSe: Thickness- and Temperature-Dependent Behaviors. *J. Phys. Chem. C* **126**, 10459–10468 (2022).

24. Wu, Y. *et al.* Quantum Confinement and Gas Sensing of Mechanically Exfoliated GaSe. *Advanced Materials Technologies* **2**, 1600197 (2017).

25. Rahaman, M., Rodriguez, R. D., Monecke, M., Lopez-Rivera, S. A. & Zahn, D. R. T. GaSe oxidation in air: from bulk to monolayers. *Semicond. Sci. Technol.* **32**, 105004 (2017).

26. Bergeron, A., Ibrahim, J., Leonelli, R. & Francoeur, S. Oxidation dynamics of ultrathin GaSe probed through Raman spectroscopy. *Applied Physics Letters* **110**, 241901 (2017).

27. Finkman, E., Tauc, J., Kershaw, R. & Wold, A. Lattice dynamics of tetrahedrally bonded semiconductors containing ordered vacant sites. *Phys. Rev. B* **11**, 3785–3794 (1975).

28. Onuma, T. *et al.* Polarized Raman spectra in β-Ga2O3 single crystals. *Journal of Crystal Growth* **401**, 330–333 (2014).

29. Becke, A. D. Density-functional thermochemistry. III. The role of exact exchange. *The Journal of Chemical Physics* **98**, 5648–5652 (1993).

30. Kranert, C., Sturm, C., Schmidt-Grund, R. & Grundmann, M. Raman tensor elements of $\beta\text{-Ga}_2\text{O}_3$. *Sci Rep* **6**, 35964 (2016).

31. Karaoglan-Bebek, G., Hwan Woo, J., Nikishin, S., Rusty Harris, H. & Holtz, M. Optical studies of the effect of oxidation on GaN. *Journal of Vacuum Science & Technology B* **32**, 011213 (2014).

32. Tang, J. *et al.* The testing of stress-sensitivity in heteroepitaxy GaN/Si by Raman spectroscopy. *Applied Surface Science* **257**, 8846–8849 (2011).

33. Huang, J. *et al.* Dislocation luminescence in GaN single crystals under nanoindentation. *Nanoscale research letters* **9**, 649 (2014).

34. Reinoso, C. *et al.* Toward a Predominant Substitutional Bonding Environment in B-Doped Single-Walled Carbon Nanotubes. *ACS Omega* **4**, 1941–1946 (2019).

35. Zhang, X., Tan, Q.-H., Wu, J.-B., Shi, W. & Tan, P.-H. Review on the Raman spectroscopy of different types of layered materials. *Nanoscale* **8**, 6435–6450 (2016).

36. Venezuela, P., Lazzeri, M. & Mauri, F. Theory of double-resonant Raman spectra in graphene: Intensity and line shape of defect-induced and two-phonon bands. *Phys. Rev. B* **84**, 035433 (2011).

37. Song, J. *et al.* Penetration depth at various Raman excitation wavelengths and stress model for Raman spectrum in biaxially-strained Si. *Sci. China Phys. Mech. Astron.* **56**, 2065–2070 (2013).

38. Diep, N. Q. *et al.* Screw-Dislocation-Driven Growth Mode in Two Dimensional GaSe on GaAs(001) Substrates Grown by Molecular Beam Epitaxy. *Sci Rep* **9**, 17781 (2019).

39. Diep, N. Q. *et al.* Pressure induced structural phase crossover of a GaSe epilayer grown under screw dislocation driven mode and its phase recovery. *Sci Rep* **11**, 19887 (2021).

40. Hoff, R. M., Irwin, J. C. & Lieth, R. M. A. Raman Scattering in GaSe. *Can. J. Phys.* **53**, 1606–1614 (1975).

41. Irwin, J. C., Hoff, R. M., Clayman, B. P. & Bromley, R. A. Long wavelength lattice vibrations in GaS and GaSe. *Solid State Communications* **13**, 1531–1536 (1973).

42. Del Pozo-Zamudio, O. *et al.* Photoluminescence and Raman investigation of stability of InSe and GaSe thin films. Preprint at http://arxiv.org/abs/1506.05619 (2015).

43. Mahjoub, M. A. *et al.* Impact of Wet Treatments on the Electrical Performance of Ge0.9Sn0.1-Based p-MOS Capacitors. *ACS Appl. Electron. Mater.* **1**, 260–268 (2019).

44. Benrabah, S. *et al.* H3PO4-based wet chemical etching for recovery of dry-etched GaN surfaces. *Applied Surface Science* **582**, 152309 (2022).

45. Fauquier, L. *et al.* Depth profiling analysis of HfON on SiON ultrathin films by parallel angle resolved x-ray photoelectron spectroscopy and medium energy ion scattering. *Surface and Interface Analysis* **48**, 436–439 (2016).

46. Cumpson, P. J. & Seah, M. P. Random uncertainties in AES and XPS: I: Uncertainties in peak energies, intensities and areas derived from peak synthesis. *Surface and Interface Analysis* **18**, 345–360 (1992).

47. Wei, C. *et al.* Bound exciton and free exciton states in GaSe thin slab. *Sci Rep* **6**, 33890 (2016).